

PRPO: PARAGRAPH-LEVEL POLICY OPTIMIZATION FOR VISION-LANGUAGE DEEPFAKE DETECTION

Tuan Nguyen¹ Naseem Khan¹ Khang Tran² NhatHai Phan² Issa Khalil¹

¹Qatar Computing Research Institute, Qatar

²New Jersey Institute of Technology, USA

{ntuan, nakh12498, ikhalil}@hbku.edu.qa, {kt36, phan}@njit.edu

ABSTRACT

The rapid rise of synthetic media has made deepfake detection a critical challenge for online safety and trust. Progress remains constrained by the scarcity of large, high-quality datasets. Although multimodal large language models (LLMs) exhibit strong reasoning capabilities, their performance on deepfake detection is poor, often producing explanations that are misaligned with visual evidence or hallucinatory. To address this limitation, we introduce a reasoning-annotated dataset for deepfake detection and propose Paragraph-level Relative Policy Optimization (PRPO), a reinforcement learning algorithm that aligns LLM reasoning with image content at the paragraph level. Experiments show that PRPO improves detection accuracy by a wide margin and achieves the highest reasoning score of 4.55/5.0. Ablation studies further demonstrate that PRPO significantly outperforms GRPO under test-time conditions. These results underscore the importance of grounding multimodal reasoning in visual evidence to enable more reliable and interpretable deepfake detection.

1 INTRODUCTION

Generative Artificial Intelligence (GAI) has advanced rapidly with the development of generative adversarial networks (GANs) [17], diffusion models [21; 64], and their variants [65; 57; 20; 22; 59]. These models, based on distribution matching, generate high-quality synthetic samples that support a wide range of applications [24; 72; 26; 50; 57; 22]. However, the same capability has fueled deepfake creation, where real and synthetic images are nearly indistinguishable [45; 40], enabling misuse in misinformation, identity theft, and challenges to authorship [30; 42; 28; 44]. Detecting deepfakes is particularly challenging because synthetic data is trained to mimic the real distribution, making decision boundaries subtle and unstable, especially for unseen models or domains. This motivates the development of detection methods that move beyond surface artifacts to leverage deeper, semantically meaningful cues for robust real-fake discrimination.

Deepfake technology has advanced rapidly, raising the bar for detection methods to be practically useful. Beyond binary classification, reliable reasoning for why an image is flagged as a deepfake is increasingly critical [76]. Multimodal Large Language Models (MLLMs) show promise for this task [36; 67; 47; 16], as their large-scale training enables them to capture semantic structures and global visual meaning. However, several challenges limit their effectiveness for deepfake detection. (i) **Data requirements:** detection is data-hungry, and fine-tuning via simple question-answer distillation [8] is inadequate, since models such as LLaVA [36] are optimized for short answers rather than detailed reasoning. (ii) **Architecture limitations:** subtle manipulations demand fine-grained visual representations that generic vision encoders often fail to capture. (iii) **Reasoning quality:** existing models frequently jump to premature conclusions, biasing subsequent reasoning and overlooking visual evidence. Ensuring systematic inspection of artifacts and progressive reasoning before prediction is thus essential for reliable detection. Figure 1 illustrates these limitations by contrasting explanations from LLaVA with those of our proposed PRPO.

In this paper, we aim to improve both the generalization ability of deepfake detection and the quality of its reasoning responses. Our main contributions are as follows:

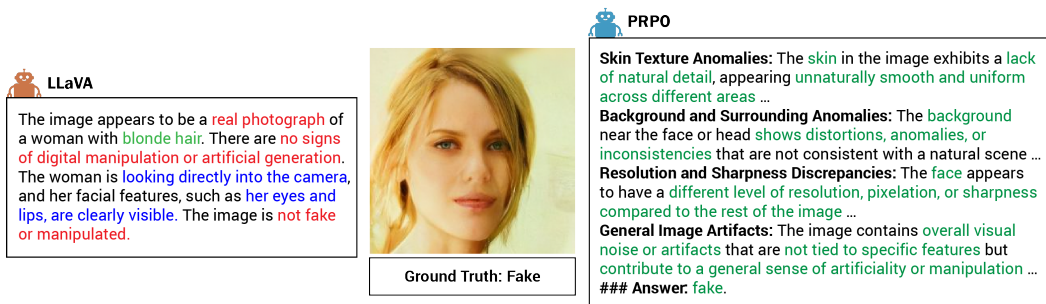


Figure 1: Reasoning quality comparison between LLaVA and the proposed PRPO. LLaVA and other MLLMs often produce surface-level predictions, yielding misleading reasoning (red) or irrelevant descriptions unrelated to deepfake detection (blue). In contrast, PRPO generates visually grounded explanations (green), describing each deepfake characteristic in a dedicated paragraph and systematically aligning reasoning with image evidence before reaching a conclusion.

- We introduce **DF-R5**, a reasoning-annotated dataset for deepfake detection containing 115k images paired with high-quality explanations, designed to enhance the reasoning capabilities of MLLMs. This dataset fills the gap in reasoning annotations and supports community research in this area.
- We design **DX-LLaVA**, a multimodal architecture for Deepfake detection and eXplainability, which integrates a CLIP ConvNeXT vision encoder with a Vicuna language model to capture fine-grained visual artifacts while leveraging strong reasoning ability.
- We propose Paragraph-level Relative Policy Optimization (**PRPO**), a novel test-time reinforcement learning algorithm that aligns MLLM reasoning with image content at the paragraph level. PRPO encourages the model to generate explanations that are not only accurate but also detailed to the visual evidence present in the images. Especially, PRPO can be applied at test time, making it a flexible solution for enhancing reasoning without requiring extensive retraining with annotated data. To the best of our knowledge, PRPO is the first reinforcement learning approach applied to deepfake detection and explainability.
- We conduct extensive experiments showing significant gains in both detection accuracy and explanation faithfulness. On unseen domains, our method achieves a 9% improvement in accuracy and a reasoning score of 4.55/5.0, surpassing Gemini's 4.2/5.0. These results highlight the importance of grounding multimodal reasoning in visual evidence for reliable and interpretable deepfake detection. Code and dataset are available at <https://github.com/tuanrpt/PRPO>.

2 RELATED WORK

Traditional Deepfake Detection The rapid progress of generative AI has made distinguishing real from synthetic images a central problem in image forensics. Modern deepfake detection targets images produced by diffusion models [21; 64], GANs [17], and related techniques, whose outputs often exhibit photo-realistic quality. Recent approaches transfer powerful vision backbones such as CLIP-ViT [12] and ConvNeXT [38] to detection tasks [61; 2; 46], or exploit frequency-domain features to capture subtle generative artifacts [15; 25; 29; 31; 56; 66]. While effective, these methods largely lack explainability, providing limited insight into the cues driving predictions.

Deepfake Detection with LLMs Large Language Models (LLMs) excel in multimodal tasks such as captioning [53; 32; 33], Visual Question Answering (VQA) [36; 37], and even image generation [57; 5; 51]. Recent work has explored fine-tuning Multimodal LLMs (MLLMs) for deepfake detection [8; 34; 19; 70; 23]. However, existing datasets rarely include detailed reasoning annotations, leading models to generate shallow explanations that overlook critical cues. Moreover, explanation quality is seldom evaluated, limiting trustworthiness. To address this gap, we introduce

a reasoning-annotated dataset for deepfake detection and a reinforcement learning framework that trains models to provide accurate, interpretable reasoning.

Test-Time Reinforcement Learning Reinforcement Learning (RL) has proven effective for improving LLM outputs [49; 54; 62; 77]. RLHF [10; 49] aligns models with human preferences via algorithms such as PPO [60] and DPO [54]. Group Relative Policy Optimization (GRPO) [62] extends this by optimizing relative quality across responses, mitigating reward sensitivity and improving stability, powering models like DeepSeek-R1 [18]. More recently, Test-Time RL (TTRL) enables models to self-improve during inference using majority voting [78] or self-certainty rewards [77], without additional training data. RL has also been applied in multimodal tasks such as captioning [55; 74] and VQA [75; 69], but remains underexplored for deepfake detection. A central challenge is designing rewards that capture both detection accuracy and fine-grained explanatory cues, which LLMs often overlook or hallucinate. Our method, PRPO, addresses this by introducing paragraph-level rewards that explicitly align explanations with visual evidence, advancing RL-driven deepfake detection and explainability.

3 METHODOLOGY

In this section, we introduce the DF-R5 dataset, a large-scale multimodal deepfake reasoning corpus constructed from state-of-the-art multimodal large language models (MLLMs) for deepfake detection. We then refine the quality of its reasoning annotations using the Paragraph-level Relative Policy Optimization (PRPO) algorithm.

3.1 REASONING DATA GENERATION

Table 1: MLLM performance (%) on 1,000 DF-R5 samples.

Model	Acc	Pre	Rec	F1
Claude-3 [3]	50.80	65.38	3.40	6.46
Pixtral [43]	51.60	71.05	5.40	10.04
LLaMA-4 [41]	64.90	73.21	47.00	57.25
Qwen-2.5 [52]	62.64	69.17	52.23	59.52
GPT-4o [48]	70.80	93.33	44.80	60.54
Gemini-2.5 [16]	77.60	75.09	82.60	78.67

DF-R5 is a multi-domain deepfake reasoning dataset containing approximately 115k image-reasoning pairs with rich semantic annotations. The base images are sourced from DF40 [71], covering five diverse generative domains: DDIM [64], PixArt- α [7], SD-2.1 [57], SiT [4], and StyleGAN3 [27]. These domains are selected to maximize both diversity and difficulty, ensuring robust generalization across generation methods.

A naive approach would be to directly distill reasoning from MLLMs using the collected images. However, two challenges arise: (1) identifying which MLLM provides the strongest reasoning quality, and (2) designing prompting strategies that can minimize hallucination and misinformation.

To address the first challenge, we systematically benchmark several representative MLLMs by asking them to classify 1,000 randomly selected images (balanced between real and fake). The results, presented in Table 1, indicate that Claude-3 and Pixtral yield high precision but fail to capture most true cues, resulting in very low recall. Gemini-2.5 achieves the best trade-off, with the highest overall accuracy (77.60%) and F1 score (78.67%), and is thus selected as the primary model for reasoning distillation.

To address the second challenge, we design a three-step pipeline, illustrated in Figure 2, to generate consistent, high-quality reasoning annotations from Gemini:

Step 1: Feature Discovery. We prompt multiple vision-language models (Gemini-2.5 [16], Qwen-2.5 [52], LLaMA-4 [41], GPT-4o [47]) to enumerate facial and visual characteristics relevant to deepfake detection. Each model proposes K candidate features (e.g., $K = 50$), yielding approximately $4 \times K$ (e.g., 200) unique features in total. Importantly, **no images are provided at this**

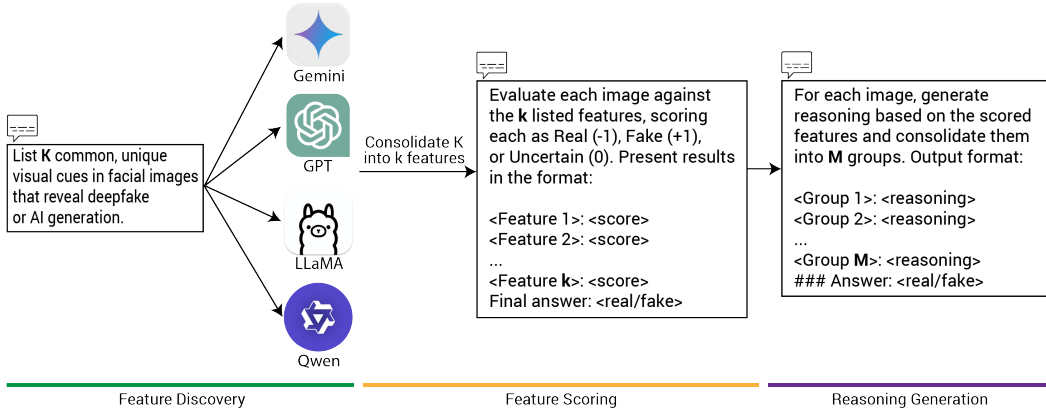


Figure 2: Three-step pipeline for generating high-quality reasoning annotations in DF-R5. The detailed prompts for each step are presented in the Appendix A.3.

stage, the prompts focus on eliciting general, commonly recognized features from the models. After deduplication and consolidation, we curate a final set of k features (e.g., $k = 74$).

Step 2: Feature Scoring. For each image, given the list of k features, we prompt Gemini to assign a score of Real (−1), Fake (+1), or Uncertain (0) to each feature. This step mitigates the risk of Gemini selecting all features indiscriminately or relying on hallucinated ones among the k candidates. Cases flagged as incorrect or uncertain are further refined through additional prompting with ground-truth labels. This procedure enhances the reliability of the predictions, as suggested by [73]. The distribution of the collected feature data is reported in Appendix A.2.

Step 3: Reasoning Generation. Each image now has a corresponding set of feature scores from Step 2. To avoid redundancy and overly lengthy explanations, we instruct Gemini to consolidate fine-grained feature scores into at most M semantically coherent groups (e.g., $M = 7$). The choice of M is guided by the 85% group frequency threshold, ensuring that the majority of commonly observed features are represented. Importantly, we do not require Gemini to map features into a fixed set of groups; instead, it is prompted to organize them into at most M groups, depending on the content of each image. This produces concise and interpretable reasoning descriptions for each image.

3.2 FINE-TUNING WITH DX-LLAVA

Table 2: Intra-domain vs. inter-domain performance (%).

Method	Acc	Prec	Rec	F1
Intra-domain	99.57	99.84	99.35	99.59
Inter-domain	59.40	98.26	21.90	35.82

In this section, we fine-tune a LLaVA-based architecture [36] on our DF-R5 dataset. We start with naive fine-tuning and progressively incorporate enhancements to improve generalization across unseen domains.

Our baseline is the original LLaVA, comprising a CLIP ViT-L/14 visual encoder [53], a Vicuna language model [9], and a multimodal projector mapping ViT patch embeddings into Vicuna’s token space. Table 2 reports results under two settings: (i) **Intra-domain**, with random train/validation/test splits, and (ii) **Inter-domain**, with one domain held out. While intra-domain accuracy exceeds 99%, inter-domain performance drops sharply: precision remains high, but the model collapses to predicting nearly all images as real. Moreover, we find that Vicuna generates coherent text yet fails to distinguish real from fake, reflecting poor alignment of the projector with discriminative visual cues. To address this, we add a lightweight classifier on top of the projector. CLIP patch

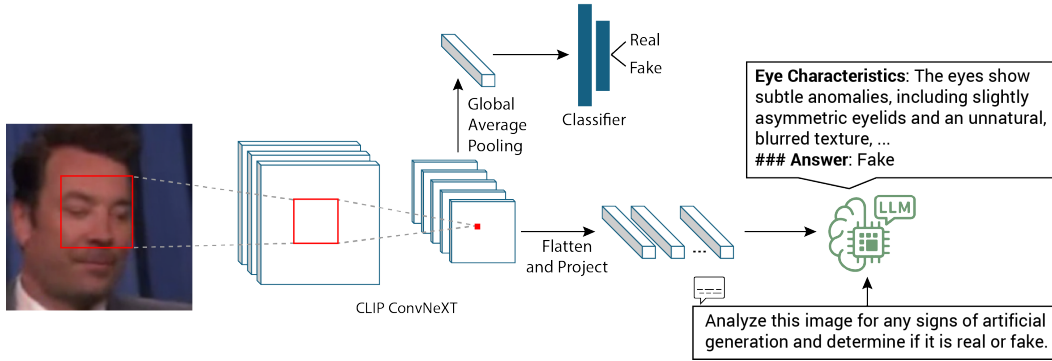


Figure 3: Proposed DX-LLaVA, a LLaVA fine-tuning framework for Deepfake detection and eXplainability. Unlike CLIP ViT, which outputs patch embeddings, CLIP ConvNeXT produces pixel-level embeddings. This enables a finer focus on local image regions, leading to improved deepfake detection and reasoning performance.

embeddings are aggregated via global average pooling (GAP) into a pooled representation \bar{e} , which is then classified:

$$e = \text{CLIP}(x) \in \mathbb{R}^{P \times d}, \quad \bar{e} = \text{GAP}(e), \quad \hat{y} = \mathcal{C}(\bar{e}; \phi). \quad (1)$$

where e denotes the patch embeddings, and \mathcal{C} the classifier parameterized by ϕ . We now train the classifier along with the projector W and Vicuna π_θ to minimize:

$$\min_{\theta, W, \phi} \mathcal{L}_{\text{total}} := \mathcal{L}_{\text{lm}} + \alpha \mathcal{L}_{\text{binary}} = \mathbb{E}_{(x, o_{<t}, o_t) \sim \mathcal{D}} [-\log \pi_\theta(o_t | o_{<t}, z)] + \alpha \mathbb{E}_{(x, y) \sim \mathcal{D}} [-y \log \hat{y}], \quad (2)$$

where $\mathcal{D} = \{(x_i, o_i, y_i)\}_{i=1}^N$ is our dataset consisting of images x_i , reasoning sequences o_i , and corresponding ground-truth labels y_i . Here, $z = e \cdot W$ denotes the projected image token input to Vicuna, and α is a trade-off parameter that balances the language modeling loss \mathcal{L}_{lm} with the binary classification loss $\mathcal{L}_{\text{binary}}$.

Table 3: Performance comparison (%) of \mathcal{L}_{lm} and $\mathcal{L}_{\text{lm}} + \alpha \mathcal{L}_{\text{binary}}$.

Method	Acc	Pre	Rec	F1
\mathcal{L}_{lm}	59.40	70.40	21.90	35.82
$\mathcal{L}_{\text{lm}} + \alpha \mathcal{L}_{\text{binary}}$	70.40	92.97	46.12	61.66

Table 3 shows that incorporating a binary loss improves detection performance and strengthens Vicuna's ability to discriminate between real and fake images. However, gains remain limited by a core weakness of LLaVA: the CLIP ViT encoder [53]. While ViT captures global semantics effective for VQA, deepfake detection demands sensitivity to local, high-frequency artifacts, making ViT suboptimal. To overcome this, we propose DX-LLaVA, which replaces CLIP ViT with CLIP ConvNeXT [1], a convolutional encoder with stronger texture bias and greater sensitivity to subtle artifacts such as hairline irregularities, pore inconsistencies, and abnormal background details (Figure 3). Specifically, we use the output from **Stage 3** of ConvNeXT, yielding a 10×10 feature map flattened into 100 pixel embeddings and projected into Vicuna's text embedding space via the projector. The objective remains as in Equation 2, with both the projector and Vicuna fine-tuned to adapt to ConvNeXT features. Detection results are reported in Table 4.

3.3 TEST-TIME DEEPFAKE DETECTION WITH PRPO

After fine-tuning, we observed two recurring issues in the generated reasoning: (i) **Image-Reason Consistency**, where explanations often failed to align with visual content, including redundant or overly generic cues not present in the image; and (ii) **Reason-Prediction Consistency**, where the

final answer occasionally contradicted the consensus of supporting paragraphs, producing incorrect outputs despite consistent evidence. These issues stem from the fact that MLLMs are generally optimized for the final decision, which can induce hallucinations in intermediate reasoning. Existing RL algorithms also focus on rewarding final outputs [62], often neglecting reasoning quality. Unlike mathematical reasoning, where step-wise evaluation is feasible [68; 11], evaluating intermediate textual reasoning in deepfake detection is more challenging. To address this gap, we propose a reinforcement learning algorithm that mitigates misinformation, enforces consistency between reasoning and predictions, and yields more reliable explanations for deepfake detection.

We propose a novel Paragraph-level Relative Policy Optimization (PRPO), inspired by the GRPO algorithm [62]. Given a prompt v and image tokens z , the policy π_θ produces a set of sampled outputs $\mathcal{O} = \{o^{(1)}, o^{(2)}, \dots, o^{(L)}\}$. Each output $o^{(i)}$ is split into $M_i + 1$ paragraphs: $o^{(i)} = \{p_1^{(i)}, p_2^{(i)}, \dots, p_{M_i+1}^{(i)}\}$, where $p_{M_i+1}^{(i)}$ denotes the final-answer sentence. To enhance the reasoning ability of DX-LLaVA, we introduce two reward functions: the Visual Consistency Reward (VCR) and the Prediction Consistency Reward (PCR).

Visual Consistency Reward (VCR). VCR enforces alignment between each paragraph $p_j^{(i)}$ and the image features. Specifically, we leverage the frozen CLIP ConvNeXT encoder in our architecture to compute alignment between image features and paragraph content. Since CLIP ConvNeXT is limited by input length, we first extract representative keywords from each paragraph using the YAKE library¹ [6]: $s = \text{YAKE}(p_j^{(i)})$. YAKE is a lightweight, unsupervised keyword extraction method requiring no external models. The reward score is then computed as:

$$R_{VCR}(p_j^{(i)}) = \frac{1}{2} [\text{sim}(s, \text{CLIP}(x)) + 1], \quad (3)$$

where $\text{sim}(\cdot, \cdot)$ denotes cosine similarity, and R_{VCR} is normalized to $[0, 1]$.

Prediction Consistency Reward (PCR). PCR evaluates the internal consistency between the majority vote of reasoning paragraphs and the final conclusion sentence $p_{M_i+1}^{(i)}$. In our dataset, we observe that all reasoning paragraphs typically agree when describing real or fake characteristics. Therefore, for intermediate paragraphs we set $R_{PCR}(p_j^{(i)}) = 1$ for simplicity. For the final paragraph, however, its reward is determined by whether its prediction matches the majority vote from the preceding paragraphs:

$$R_{PCR}(p_{M_i+1}^{(i)}) = \begin{cases} 1.0 & \text{if } \arg \max_{\ell \in \{\text{real,fake}\}} |\{j < M_i + 1 : \hat{y}(p_j^{(i)}) = \ell\}| = \hat{y}(p_{M_i+1}^{(i)}), \\ 0.0 & \text{otherwise.} \end{cases}$$

Here, $\hat{y}(p_j^{(i)})$ denotes the label predicted for paragraph $p_j^{(i)}$ using predefined dictionaries of deepfake-related terms $\mathcal{F} = \{\text{unnatural, inconsistent, manipulated, overly smooth, ...}\}$, real terms $\mathcal{R} = \{\text{authentic, genuine, realistic, natural, ...}\}$, and negation terms $\mathcal{N} = \{\text{no, not, without, lack of, ...}\}$. The procedure for reward computation is presented in Algorithms 1, 2, and 3 in Appendix A.5. We find that this approach effectively mitigates the consistency problem while avoiding reliance on external models and additional computational overhead.

The overall reward for a paragraph is defined as the average of the two reward components:

$$R(p_j^{(i)}) = \frac{1}{2} (R_{VCR}(p_j^{(i)}) + R_{PCR}(p_j^{(i)})). \quad (4)$$

where $j = 1, 2, \dots, M + 1$. The core idea of our reward function design is to leverage **self-consistency** and **visual grounding** without requiring paragraph-level supervision. Importantly, the final prediction does not depend on ground-truth labels. By employing such label-free rewards, the model is encouraged to generalize more effectively to unseen images. For each group \mathcal{O} , we compute the mean μ_R and standard deviation σ_R of rewards across all paragraphs. The normalized relative advantage of paragraph $p_j^{(i)}$ is defined as $A_j^{(i)} = \frac{R(p_j^{(i)}) - \mu_R}{\sigma_R + \epsilon}$, where ϵ is a small constant added for numerical stability.

¹<https://github.com/LIAAD/yake>

Given a prompt v and image tokens z , PRPO maximizes the log-probabilities of paragraphs weighted by their own relative advantage, with PPO-style clipping for stability:

$$\mathcal{L}_{\text{PRPO}}(\theta) = \mathbb{E}_{\mathcal{O} \sim \pi_\theta} \left[\sum_{i=1}^L \sum_{j=1}^{M_i+1} \min \left(\frac{\pi_\theta(p_j^{(i)} | v, z)}{\pi_{\text{old}}(p_j^{(i)} | v, z)} A_j^{(i)}, \text{clip} \left(\frac{\pi_\theta(p_j^{(i)} | v, z)}{\pi_{\text{old}}(p_j^{(i)} | v, z)}, 1 - \epsilon, 1 + \epsilon \right) A_j^{(i)} \right) \right]. \quad (5)$$

Different from GRPO, where each token is treated with the same advantage, PRPO computes advantages at the paragraph level. This increases the likelihood of paragraphs (deepfake characteristics) that align with the image and remain consistent with the final answer, while decreasing the likelihood of those that are misaligned. Training also incorporates a Kullback-Leibler (KL) divergence loss to encourage exploration of novel reasoning traces at the paragraph level while constraining the policy from deviating excessively from the reference model.

$$\mathcal{L}_{\text{KL}}(\theta) = \frac{1}{\sum_{i=1}^L (M_i + 1)} \sum_{i=1}^L \sum_{j=1}^{M_i+1} \mathbb{E}_{p_j^{(i)} \sim \pi_\theta} \left[\log \frac{\pi_\theta(p_j^{(i)} | v, z)}{\pi_{\text{ref}}(p_j^{(i)} | v, z)} \right]. \quad (6)$$

The overall training objective combines the PRPO loss with the KL regularization term:

$$\mathcal{L}_{\text{total}}(\theta) = \mathcal{L}_{\text{PRPO}}(\theta) + \beta \mathcal{L}_{\text{KL}}(\theta), \quad (7)$$

where β is a weighting coefficient.

4 EXPERIMENT

4.1 SET UP

Dataset. We construct our dataset from DF-40 [71], which integrates widely used deepfake benchmarks such as FaceForensics++ [58], and CelebDF [35]. To generate synthetic images, we employ generative models including DDIM [64], PixArt [7], SD-2.1 [57], SiT-XL/2 [4], and StyleGAN [27]. For each domain, we collect 30k images, resulting in 150k samples in total. After filtering invalid formats with Gemini, the final dataset contains around 115k images.

Implementation Details. We fine-tune the DX-LLaVA model by optimizing the objective in Eq. (2) with $\alpha = 10.0$. For reasoning with PRPO, we set $\beta = 0.01$ in Eq. (7). A pretrained LLaVA-7B is used, where the CLIP ConvNeXT backbone [1] is frozen. Images are resized to 320×320 and processed with the default CLIP pipeline [53]. The CLIP pixel-level embeddings (1536 dimensions) are projected to 4096 dimensions to match Vicuna’s text embedding space. We use a learning rate of 2×10^{-5} for fine-tuning and 3×10^{-7} for PRPO-based reasoning with the `ver1` package [63]. Training is distributed across multiple GPUs, enabling parallel reward computation and YAKE-based token extraction. All tasks adopt the same settings and are optimized with AdamW [39]. Experiments are conducted on 8 NVIDIA H200 GPUs, each with 143 GB of memory.

4.2 GENERALIZATION RESULTS

Table 4 reports detection accuracy against deepfake detection baselines, including LLaVA [36], DE-FAKE [61], FakeShield [70], UnivCLIP [46], and SIDA [23]. DX-LLaVA achieves an average accuracy of 78.08%, outperforming state-of-the-art baselines (e.g., improving upon SIDA by 3%). Incorporating PRPO boosts performance to 89.91%, setting a new state of the art and outperforming SIDA by 14%. PRPO is particularly effective in challenging domains such as SiT where real and fake images are nearly indistinguishable, demonstrating its robustness. Additional metrics (accuracy, precision, recall) are provided in Table 10 in the Appendix. Table 5 compares our method against recent MLLMs, including LLaMA-4 Maverick [41], Pixtral-12B [43], Qwen2.5-VL-32B [52], GPT-4o [47], Gemma-3-27B-IT [13], and Gemini-2.5 [16]. Although DX-LLaVA benefits from Gemini distillation, its accuracy remains 2% below Gemini-2.5, suggesting that larger-scale data or stronger reasoning may be required. In contrast, PRPO achieves 89.91%, significantly surpassing MLLM baselines, with Gemini-2.5 the closest competitor. These results demonstrate the effectiveness of PRPO in advancing deepfake detection beyond both state-of-the-art baselines and MLLMs.

Table 4: Detection performance (F1 score, %) of our method versus baselines. $\rightarrow X$ denotes testing on unseen domain X , with the remaining four domains used for training.

Method	\rightarrow DDIM	\rightarrow PixArt	\rightarrow SD	\rightarrow SiT	\rightarrow StyleGAN	Average
LLaVA	49.86	65.46	26.54	15.36	57.03	42.85
DE-FAKE	8.83	86.45	95.80	4.55	76.50	54.43
FakeShield	31.84	88.57	92.28	33.22	98.70	68.92
UnivCLIP	74.85	89.31	74.81	40.01	86.46	73.09
SIDA	70.07	73.86	92.37	46.53	94.98	75.26
DX-LLaVA (ours)	92.34	83.11	89.35	26.46	99.13	78.08
PRPO (ours)	95.88	88.10	94.99	71.26	99.32	89.91

Table 5: Average detection performance (%) of MLLMs across five domains.

Model	Acc	Pre	Rec	F1
LLaMA-4 Maverick	53.58	73.29	14.59	23.23
Pixtral-12B	63.27	69.61	36.85	44.38
Qwen2.5-VL-32B	59.54	64.87	59.54	54.18
GPT-4o	57.96	73.38	57.96	63.11
Gemma-3-27B-IT	66.44	65.69	70.55	67.64
Gemini-2.5	85.00	94.23	74.44	80.31
DX-LLaVA (ours)	84.64	99.57	70.58	78.08
PRPO (ours)	89.02	91.40	89.42	89.91

4.3 EXPLANATION QUALITY EVALUATION

Table 6 presents the explanation quality scores assigned by GPT-4o across five key criteria, drawing inspiration from the evaluation methodologies of [14] and [70]. For each criterion, GPT-4o rates the explanations on a scale from 1 to 5: (i) **Classification Accuracy and Consistency (CAC)**: correctly classifying the image as real or fake while remaining consistent with the ground truth; (ii) **Evidence Grounding and Image Alignment (EGIA)**: citing visual artifacts that are actually present in the image and avoiding hallucinations; (iii) **Reasoning Quality (RQ)**: providing step-by-step explanations free of contradictions or irrelevant details; (iv) **Confidence Calibration (CC)**: expressing confidence at a level appropriate to the evidence, without overstating or understating certainty; and (v) **Clarity and Usefulness (CU)**: producing clear, well-structured, and interpretable explanations that are useful for human investigators. The detailed prompt is shown in Figure 9 in the Appendix.

We compare our method against several MLLM baselines. Our fine-tuned DX-LLaVA model achieves an overall score of 4.02, outperforming most baselines except Gemini-2.5 (4.20). With PRPO, the score rises substantially to 4.55/5.0, surpassing all baselines by a notable margin. PRPO shows particular strength in CAC and EGIA, highlighting its ability to align reasoning with image features and maintain consistency in prediction, thereby improving deepfake detection accuracy and producing high-quality, reliable explanations.

4.4 ABLATION STUDY ON REWARD COMPONENTS

Table 7 reports ablation results on reward components for transfer to the **SD** domain. Using only the Visual Consistency Reward (VCR) achieves very high precision (99.30%) but low recall (80.11%), while using only the Prediction Consistency Reward (PCR) further reduces recall to 55.11%. These results show that each reward alone is insufficient: VCR mitigates hallucinations but lacks decision-level alignment, whereas PCR enforces alignment but encourages overly generic or systematically incorrect predictions due to the absence of visual grounding. Combining both rewards yields balanced gains, boosting recall to 93.37% while maintaining strong precision (96.67%), and producing the best F1 score (94.99%).

Table 6: Reasoning quality evaluation conducted by GPT-4o.

Model	CAC	EGIA	RQ	CC	CU	Overall
GPT-4o-Mini	2.98	1.32	1.94	2.67	2.99	2.38
LLaVA-Base	3.07	2.76	2.92	3.18	3.94	3.17
LLaMA-4-Maverick	2.70	3.34	3.26	3.01	4.06	3.27
Pixtral-12B	3.17	3.51	3.40	3.38	4.20	3.53
Qwen2.5-VL-32B	3.02	3.70	3.64	3.28	4.29	3.59
Gemma-3-27B-IT	3.36	3.77	3.76	3.51	4.42	3.76
Gemini-2.5	3.98	4.16	4.23	4.05	4.60	4.20
DX-LLaVA (ours)	3.78	3.99	4.04	3.98	4.29	4.02
PRPO (ours)	4.42	4.56	4.58	4.50	4.69	4.55

Table 7: Performance comparison (%) of different reward components on transfer task → **SD**.

Method	Acc	Prec	Rec	F1
VCR only	89.20	99.30	80.11	88.68
PCR only	76.20	99.66	55.11	70.98
Full rewards	94.80	96.67	93.37	94.99

4.5 ABLATION STUDY ON OTHER RL METHODS

We compare our PRPO framework with other RL algorithms adapted for test-time optimization, including PPO [60] and GRPO [62] from Test-Time Reinforcement Learning (TTRL) [78]. In TTRL, the authors apply majority voting at the sample level, using the final answer as the prediction. As shown in Table 8, PPO achieves high precision (99.79%) but lower recall (88.76%), reflecting its tendency to produce overly conservative predictions that miss many true positives. GRPO, on the other hand, achieves perfect precision (100.0%) but with slightly lower recall than PPO, suggesting an even stronger bias toward cautious predictions. In contrast, our PRPO method provides the best overall balance, attaining the highest accuracy (95.80%), recall (93.14%), and F1 score (95.88%), while maintaining strong precision (98.79%). PRPO is specifically designed to capture self-consistency between visual cues and reasoning at the paragraph level, highlighting the importance of fine-grained alignment for reliable deepfake detection and explainability.

Table 8: Performance comparison (%) of different RL methods on transfer task → **DDIM**.

Method	Acc	Pre	Rec	F1
DX-LLaVA (ours)	92.60	99.11	86.43	92.34
PPO (TTRL)	94.00	99.79	88.76	93.95
GRPO (TTRL)	92.29	100.00	85.33	92.09
PRPO (ours)	95.80	98.79	93.14	95.88

5 CONCLUSION

This work addresses the critical challenge of deepfake detection in the era of synthetic media, where explaining *why* an image is classified as real or fake is as important as the classification itself. We introduce a reasoning-annotated dataset, a multimodal architecture for deepfake detection and explainability, and Paragraph-level Relative Policy Optimization (PRPO), a reinforcement learning algorithm that enhances the reasoning capabilities of multimodal large language models (MLLMs) by aligning their explanations with visual evidence at a granular level. PRPO encourages models to generate detailed, evidence-grounded explanations without requiring extensive retraining on annotated data. Extensive experiments demonstrate that our approach substantially improves both detection accuracy and explanation faithfulness. PRPO paves the way for future research on integrating structured reasoning with vision-language models in safety-critical applications.

REFERENCES

- [1] Clip convnext-large-d 320: Laion-2b s29b b131k fine-tuned (soup) – hugging face, September 2023. URL https://huggingface.co/laion/CLIP-convnext_large_d_320.laion2B-s29B-b131K-ft-soup.
- [2] Sifat Muhammad Abdullah, Aravind Cheruvu, Shravya Kanchi, Taejoong Chung, Peng Gao, Murtuza Jadliwala, and Bimal Viswanath. An analysis of recent advances in deepfake image detection in an evolving threat landscape. In *2024 IEEE Symposium on Security and Privacy (SP)*, pp. 91–109, 2024. doi: 10.1109/SP54263.2024.00194.
- [3] Anthropic. The claude 3 model family: Opus, sonnet, haiku. <https://www.anthropic.com/claude-3-model-card>, 2024. Model announced on March 4, 2024.
- [4] Sara Atito, Muhammad Awais, and Josef Kittler. SiT: Self-supervised vision transformer. *arXiv preprint arXiv:2104.03602*, 2021.
- [5] James Betker, Gabriel Goh, Li Jing, Tim Brooks, Jianfeng Wang, Linjie Li, Long Ouyang, Juntang Zhuang, Joyce Lee, Yufei Guo, Wesam Manassra, Prafulla Dhariwal, Casey Chu, Yunxin Jiao, and Aditya Ramesh. Improving image generation with better captions, 2023.
- [6] Ricardo Campos, Vítor Mangaravite, Arian Pasquali, Alípio Jorge, Célia Nunes, and Adam Jatowt. YAKE!: Keyword extraction from single documents using multiple local features. *Information Sciences*, 509:257–289, 2020.
- [7] Junsong Chen, Jincheng YU, Chongjian GE, Lewei Yao, Enze Xie, Zhongdao Wang, James Kwok, Ping Luo, Huchuan Lu, and Zhenguo Li. Pixart-\$\alpha\$: Fast training of diffusion transformer for photorealistic text-to-image synthesis. In *The Twelfth International Conference on Learning Representations (ICLR)*, 2024.
- [8] Yize Chen, Zhiyuan Yan, Siwei Lyu, and Baoyuan Wu. X²-DFD: A framework for explainable and extendable deepfake detection. *arXiv preprint arXiv:2410.06126*, 2024.
- [9] Wei-Lin Chiang, Zhuohan Li, Zi Lin, Ying Sheng, Zhanghao Wu, Hao Zhang, Lianmin Zheng, Siyuan Zhuang, Yonghao Zhuang, Joseph E. Gonzalez, Ion Stoica, and Eric P. Xing. Vicuna: An open-source chatbot impressing gpt-4 with 90%* chatgpt quality. <https://lmsys.org/blog/2023-03-30-vicuna/>, March 2023.
- [10] Paul F Christiano, Jan Leike, Tom B Brown, Miljan Martic, Shane Legg, and Dario Amodei. Deep reinforcement learning from human preferences. In *Advances in Neural Information Processing Systems*, volume 30, pp. 4299–4307, 2017.
- [11] Ganqu Cui, Lifan Yuan, Zefan Wang, Hanbin Wang, Wendi Li, Bingxiang He, Yuchen Fan, Tianyu Yu, Qixin Xu, Weize Chen, Jiarui Yuan, Huayu Chen, Kaiyan Zhang, Xingtai Lv, Shuo Wang, Yuan Yao, Xu Han, Hao Peng, Yu Cheng, Zhiyuan Liu, Maosong Sun, Bowen Zhou, and Ning Ding. PROCESS REINFORCEMENT THROUGH IMPLICIT REWARDS. *arXiv preprint arXiv:2502.01456*, 2025. URL <https://arxiv.org/abs/2502.01456>.
- [12] Alexey Dosovitskiy, Lucas Beyer, Alexander Kolesnikov, Dirk Weissenborn, Xiaohua Zhai, Thomas Unterthiner, Mostafa Dehghani, Matthias Minderer, Georg Heigold, Sylvain Gelly, Jakob Uszkoreit, and Neil Houlsby. An image is worth 16x16 words: Transformers for image recognition at scale. In *International Conference on Learning Representations (ICLR)*, 2021.
- [13] Gemma Team et al. Gemma 3 technical report, 2025.
- [14] Niki M Foteinopoulou, Enjie Ghorbel, and Djamila Aouada. A hitchhiker’s guide to fine-grained face forgery detection using common sense reasoning. In *Advances in Neural Information Processing Systems*, volume 37, pp. 2943–2976, 2025.
- [15] Joel Frank, Thorsten Eisenhofer, Lea Schönherr, Asja Fischer, Dorothea Kolossa, and Thorsten Holz. Leveraging frequency analysis for deep fake image recognition. In *Proceedings of the 37th International Conference on Machine Learning*, pp. 3247–3258. PMLR, November 2020.
- [16] Gemini Team. Gemini: A family of highly capable multimodal models, 2023.

[17] Ian J. Goodfellow, Jean Pouget-Abadie, Mehdi Mirza, Bing Xu, David Warde-Farley, Sherjil Ozair, Aaron Courville, and Yoshua Bengio. Generative adversarial networks, June 2014.

[18] Daya Guo, Dejian Yang, Haowei Zhang, Junxiao Song, Ruoyu Zhang, Runxin Xu, Qihao Zhu, Shirong Ma, Peiyi Wang, Xiao Bi, et al. Deepseek-r1: Incentivizing reasoning capability in llms via reinforcement learning, 2025.

[19] Haomian He, Xuelin Zhao, Yuhang Gao, Zhengchao Huang, and Bin Xia. Ffaa: Multimodal large language model based explainable open-world face forgery analysis assistant. *arXiv preprint arXiv:2408.10072*, 2024.

[20] Jonathan Ho and Tim Salimans. Classifier-free diffusion guidance. In *NeurIPS 2021 Workshop on Deep Generative Models and Causal Reasoning*, 2022.

[21] Jonathan Ho, Ajay Jain, and Pieter Abbeel. Denoising diffusion probabilistic models. In *Advances in Neural Information Processing Systems*, volume 33, pp. 6840–6851, 2020.

[22] Jonathan Ho, Niki Kalchbrenner, Robert Weichwald, Andreas Weiskopf, Prafulla Dhariwal, Ajay Jain, Christian Kütter, and Tim Salimans. Video diffusion models. *arXiv preprint arXiv:2204.03682*, 2022.

[23] Zhenglin Huang, Jinwei Hu, Xiangtai Li, Yiwei He, Xingyu Zhao, Bei Peng, Baoyuan Wu, Xiaowei Huang, and Guangliang Cheng. SIDA: social media image deepfake detection, localization and explanation with large multimodal model. In *IEEE/CVF Conference on Computer Vision and Pattern Recognition (CVPR) 2025*, 2025.

[24] Phillip Isola, Jun-Yan Zhu, Tinghui Zhou, and Alexei A Efros. Image-to-image translation with conditional adversarial networks. In *Proceedings of the IEEE conference on computer vision and pattern recognition*, pp. 112–120, 2017.

[25] Liming Jiang, Bo Dai, Wayne Wu, and Chen Change Loy. Focal frequency loss for image reconstruction and synthesis. In *2021 IEEE/CVF International Conference on Computer Vision (ICCV)*, pp. 13899–13909, Montreal, QC, Canada, October 2021. IEEE. ISBN 978-1-6654-2812-5.

[26] Tero Karras, Samuli Laine, and Timo Aila. A style-based generator architecture for generative adversarial networks, March 2019.

[27] Tero Karras, Miika Aittala, Samuli Laine, Erik Härkönen, Janne Hellsten, Jaakko Lehtinen, and Timo Aila. Alias-Free Generative Adversarial Networks. In *Advances in Neural Information Processing Systems*, volume 34, pp. 852–863, 2021.

[28] Jan Kietzmann, Linda W. Lee, Ian P. McCarthy, and Tim C. Kietzmann. Deepfakes: Trick or treat? *Business Horizons*, 63(2):135–146, March 2020.

[29] Gwanhyeong Koo, Sunjae Yoon, Ji Woo Hong, and Chang D. Yoo. Flexiedit: Frequency-aware latent refinement for enhanced non-rigid editing, July 2024.

[30] Pavel Korshunov and Sebastien Marcel. Deepfakes: a new threat to face recognition? assessment and detection, December 2018.

[31] Hanzhe Li, Yuezun Li, Jiaran Zhou, Bin Li, and Junyu Dong. Freqblender: Enhancing deepfake detection by blending frequency knowledge, May 2024.

[32] Junnan Li, Dongxu Li, Caiming Xiong, and Steven Hoi. Blip: Bootstrapping language-image pre-training for unified vision-language understanding and generation. In *Proceedings of the 39th International Conference on Machine Learning (ICML)*, pp. 12888–12900. PMLR, June 2022.

[33] Junnan Li, Dongxu Li, Silvio Savarese, and Steven Hoi. BLIP-2: Bootstrapping language-image pre-training with frozen image encoders and large language models. In *Proceedings of the 40th International Conference on Machine Learning (ICML)*, volume 202 of *Proceedings of Machine Learning Research*, pp. 19730–19742. PMLR, 23–29 Jul 2023.

[34] Yixuan Li, Xuelin Liu, Xiaoyang Wang, Shiqi Wang, and Weisi Lin. Fakelbench: Probing explainable fake image detection via large multimodal models. *arXiv preprint arXiv:2404.13306*, 2024.

[35] Yuezun Li, Xin Yang, Pu Sun, Honggang Qi, and Siwei Lyu. Celeb-df: A large-scale challenging dataset for deepfake forensics. In *Proceedings of the IEEE/CVF Conference on Computer Vision and Pattern Recognition (CVPR)*, 2020.

[36] Haotian Liu, Chunyuan Li, Qingyang Wu, and Yong Jae Lee. Visual instruction tuning. In *Advances in Neural Information Processing Systems*, volume 36, 2023.

[37] Haotian Liu, Chunyuan Li, Yuheng Li, and Yong Jae Lee. Improved baselines with visual instruction tuning. In *Proceedings of the IEEE/CVF Conference on Computer Vision and Pattern Recognition (CVPR)*, pp. 286–295, 2024.

[38] Zhuang Liu, Hanzi Mao, Chao-Yuan Wu, Christoph Feichtenhofer, Trevor Darrell, and Saining Xie. A convnet for the 2020s. In *Proceedings of the IEEE/CVF Conference on Computer Vision and Pattern Recognition (CVPR)*, pp. 11976–11986, 2022.

[39] Ilya Loshchilov and Frank Hutter. Decoupled weight decay regularization. In *International Conference on Learning Representations (ICLR)*, 2019. URL <https://openreview.net/forum?id=Bkg6RiCqY7>.

[40] Zeyu Lu, Di Huang, Jingjing Qu, Chengyue Wu, and Wanli Ouyang. Benchmarking human and model perception of ai-generated images. In *Advances in Neural Information Processing Systems*, volume 36, 2023.

[41] Meta AI. The llama 4 herd: The beginning of a new era of natively multimodal intelligence. <https://ai.meta.com/blog/llama-4-multimodal-intelligence/>, April 2025.

[42] Yisroel Mirsky and Wenke Lee. The creation and detection of deepfakes: A survey, September 2020.

[43] Mistral AI Team. Pixtral 12b. *arXiv preprint arXiv:2410.07073*, 2024. URL <https://arxiv.org/abs/2410.07073>.

[44] Thanh Thi Nguyen, Quoc Viet Hung Nguyen, Dung Tien Nguyen, Duc Thanh Nguyen, Thien Huynh-The, Saeid Nahavandi, Thanh Tam Nguyen, Quoc-Viet Pham, and Cuong M. Nguyen. Deep learning for deepfakes creation and detection: A survey, August 2022.

[45] Sophie J Nightingale and Hany Farid. Ai-synthesized faces are indistinguishable from real faces and more trustworthy. *Proceedings of the National Academy of Sciences*, 119(8):e2120481119, 2022.

[46] Utkarsh Ojha, Yuheng Li, and Yong Jae Lee. Towards universal fake image detectors that generalize across generative models. In *Proceedings of the IEEE/CVF Conference on Computer Vision and Pattern Recognition (CVPR)*, pp. 24480–24489, June 2023.

[47] OpenAI. Gpt-4 technical report, 2024.

[48] OpenAI. Hello GPT-4o. <https://openai.com/index/hello-gpt-4o/>, May 2024.

[49] Long Ouyang, Jeffrey Wu, Xu Jiang, Diogo Almeida, Carroll L. Wainwright, Pamela Mishkin, Chong Zhang, Sandhini Agarwal, Katarina Slama, Alex Ray, John Schulman, Jacob Hilton, Fraser Kelton, Luke E. Miller, Maddie Simens, Amanda Askell, Peter Welinder, Paul Francis Christiano, Jan Leike, and Ryan J. Lowe. Training language models to follow instructions with human feedback. In S. Koyejo, S. Mohamed, A. Agarwal, D. Belgrave, Y. Cho, and A. Oh (eds.), *Advances in Neural Information Processing Systems*, volume 35, pp. 27730–27744, 2022.

[50] Or Patashnik, Zongze Wu, Eli Shechtman, Daniel Cohen-Or, and Dani Lischinski. Styleclip: Text-driven manipulation of stylegan imagery. In *2021 IEEE/CVF International Conference on Computer Vision (ICCV)*, pp. 2065–2074, Montreal, QC, Canada, October 2021. IEEE. ISBN 978-1-6654-2812-5.

[51] Dustin Podell, Zion English, Kyle Lacey, Andreas Blattmann, Tim Dockhorn, Jonas Müller, Joe Penna, and Robin Rombach. Sdxl: Improving latent diffusion models for high-resolution image synthesis. In *The Twelfth International Conference on Learning Representations (ICLR)*, 2024.

[52] Qwen Team. Qwen2.5 Technical Report. *arXiv preprint arXiv:2412.15115*, 2024. URL <https://arxiv.org/abs/2412.15115>.

[53] Alec Radford, Jong Wook Kim, Chris Hallacy, Aditya Ramesh, Gabriel Goh, Sandhini Agarwal, Girish Sastry, Amanda Askell, Pamela Mishkin, Jack Clark, Gretchen Krueger, and Ilya Sutskever. Learning transferable visual models from natural language supervision. In *Proceedings of the 38th International Conference on Machine Learning (ICML)*, pp. 8748–8763. PMLR, July 2021.

[54] Rafael Rafailov, Archit Sharma, Eric Mitchell, Stefano Ermon, Christopher D. Manning, and Chelsea Finn. Direct preference optimization: Your language model is secretly a reward model, 2023.

[55] Zhou Ren, Xiaoyu Wang, Ning Zhang, Xutao Lv, and Li-Jia Li. Deep reinforcement learning-based image captioning with embedding reward. In *The IEEE Conference on Computer Vision and Pattern Recognition (CVPR)*, pp. 1151–1159, 2017.

[56] Jonas Ricker, Simon Damm, Thorsten Holz, and Asja Fischer. Towards the detection of diffusion model deepfakes. In *International Joint Conference on Computer Vision, Imaging and Computer Graphics Theory and Applications (VISIGRAPP)*, pp. 446–457, 01 2024.

[57] Robin Rombach, Andreas Blattmann, Dominik Lorenz, Patrick Esser, and Björn Ommer. High-resolution image synthesis with latent diffusion models. In *Proceedings of the IEEE/CVF Conference on Computer Vision and Pattern Recognition (CVPR)*, pp. 10684–10695, June 2022.

[58] Andreas Rossler, Davide Cozzolino, Luisa Verdoliva, Christian Riess, Justus Thies, and Matthias Niessner. FaceForensics++: Learning to Detect Manipulated Facial Images . In *2019 IEEE/CVF International Conference on Computer Vision (ICCV)*, pp. 1–11, Los Alamitos, CA, USA, November 2019. IEEE Computer Society.

[59] Tim Salimans and Jonathan Ho. Progressive distillation for fast sampling of diffusion models. In *International Conference on Learning Representations*, 2022.

[60] John Schulman, Filip Wolski, Prafulla Dhariwal, Alec Radford, and Oleg Klimov. Proximal policy optimization algorithms, 2017.

[61] Zeyang Sha, Zheng Li, Ning Yu, and Yang Zhang. De-fake: Detection and attribution of fake images generated by text-to-image generation models. In *Proceedings of the 2023 ACM SIGSAC Conference on Computer and Communications Security (CCS)*, pp. 3418–3432, New York, NY, USA, 2023. Association for Computing Machinery.

[62] Zhihong Shao, Peiyi Wang, Qihao Zhu, Runxin Xu, Junxiao Song, Xiao Bi, Haowei Zhang, Mingchuan Zhang, Y.K. Li, Y. Wu, and Daya Guo. DeepSeekMath: Pushing the limits of mathematical reasoning in open language models. *arXiv preprint arXiv:2402.03300*, 2024. URL <https://arxiv.org/abs/2402.03300>.

[63] Guangming Sheng, Chi Zhang, Zilingfeng Ye, Xibin Wu, Wang Zhang, Ru Zhang, Yanghua Peng, Haibin Lin, and Chuan Wu. Hybridflow: A flexible and efficient rlhf framework. In *Proceedings of the 20th European Conference on Computer Systems, EuroSys '25*, pp. 303–319, New York, NY, USA, 2025. Association for Computing Machinery. ISBN 9798400707742.

[64] Jiaming Song, Chenlin Meng, and Stefano Ermon. Denoising diffusion implicit models. In *International Conference on Learning Representations (ICLR)*, 2021.

[65] Yang Song, Jascha Sohl-Dickstein, Diederik P Kingma, Abhishek Kumar, Stefano Ermon, and Ben Poole. Score-based generative modeling through stochastic differential equations. In *International Conference on Learning Representations*, 2021.

[66] Chuangchuang Tan, Yao Zhao, Shikui Wei, Guanghua Gu, Ping Liu, and Yunchao Wei. Frequency-aware deepfake detection: Improving generalizability through frequency space learning, March 2024.

[67] Hugo Touvron, Thibaut Lavril, Gautier Izacard, Xavier Martinet, Marie-Anne Lachaux, Timothée Lacroix, Baptiste Rozière, Naman Goyal, Eric Hambro, Faisal Azhar, Aurélien Rodriguez, Armand Joulin, Edouard Grave, and Guillaume Lample. Llama: Open and efficient foundation language models. *arXiv preprint arXiv:2302.13971*, 2023.

[68] Peiyi Wang, Lei Li, Zhihong Shao, R. X. Xu, Damai Dai, Yifei Li, Deli Chen, Y. Wu, and Zhipang Sui. MATH-SHEPHERD: Verify and reinforce LLMs step-by-step without human annotations. In *Proceedings of the 62nd Annual Meeting of the Association for Computational Linguistics (Volume 1: Long Papers)*, pp. 9426–9439. Association for Computational Linguistics, 2024. URL <https://aclanthology.org/2024.acl-long.510/>.

[69] Jiaer Xia, Yuhang Zang, Peng Gao, Yixuan Li, and Kaiyang Zhou. Visionary-r1: Mitigating shortcuts in visual reasoning with reinforcement learning, 2025.

[70] Zhipei Xu, Xuanyu Zhang, Runyi Li, Zecheng Tang, Qing Huang, and Jian Zhang. Fakeshield: Explainable image forgery detection and localization via multi-modal large language models. In *The Thirteenth International Conference on Learning Representations*, 2025.

[71] Zhiyuan Yan, Taiping Yao, Shen Chen, Yandan Zhao, Xinghe Fu, Junwei Zhu, Donghao Luo, Chengjie Wang, Shouhong Ding, Yunsheng Wu, and Li Yuan. Df40: Toward next-generation deepfake detection. In *Advances in Neural Information Processing Systems*, 2024.

[72] Xun Yi, Esther Walia, and Mohammed Babar. Generative adversarial networks for medical image synthesis: A review. *Medical Image Analysis*, 51:1–18, 2019.

[73] Eric Zelikman, Yuhuai Wu, Jesse Mu, and Noah D. Goodman. Star: Bootstrapping reasoning with reasoning. In *Advances in Neural Information Processing Systems*, volume 35, pp. 39114–39129, 2022.

[74] Lin Zhang, Xianfang Zeng, Kangcong Li, Gang Yu, and Tao Chen. Sc-captioner: Improving image captioning with self-correction by reinforcement learning, 2025.

[75] Ruohong Zhang, Bowen Zhang, Yanghao Li, Haotian Zhang, Zhiqing Sun, Zhe Gan, Yinfei Yang, Ruoming Pang, and Yiming Yang. Improve vision language model chain-of-thought reasoning. In *Proceedings of the 63rd Annual Meeting of the Association for Computational Linguistics (ACL)*, 2025.

[76] Yue Zhang, Ben Colman, Xiao Guo, Ali Shahriyari, and Gaurav Bharaj. Common sense reasoning for deepfake detection. In *European Conference on Computer Vision (ECCV)*, 2024.

[77] Xuandong Zhao, Zhewei Kang, Aosong Feng, Sergey Levine, and Dawn Song. Learning to reason without external rewards, 2025.

[78] Yuxin Zuo, Kaiyan Zhang, Li Sheng, Shang Qu, Ganqu Cui, Xuekai Zhu, Haozhan Li, Yuchen Zhang, Xinwei Long, Ermo Hua, Biqing Qi, Youbang Sun, Zhiyuan Ma, Lifan Yuan, Ning Ding, and Bowen Zhou. Ttrl: Test-time reinforcement learning, 2025.

A APPENDIX

A.1 THE USE OF LARGE LANGUAGE MODELS (LLMs)

In this work, we acknowledge the use of ChatGPT (GPT-5) for writing assistance, particularly in polishing the manuscript and improving grammatical accuracy. The language model was also helpful in condensing text to ensure the paper fit within the page limit. All technical contributions, including experimental design, implementation, remain solely the work of the authors.

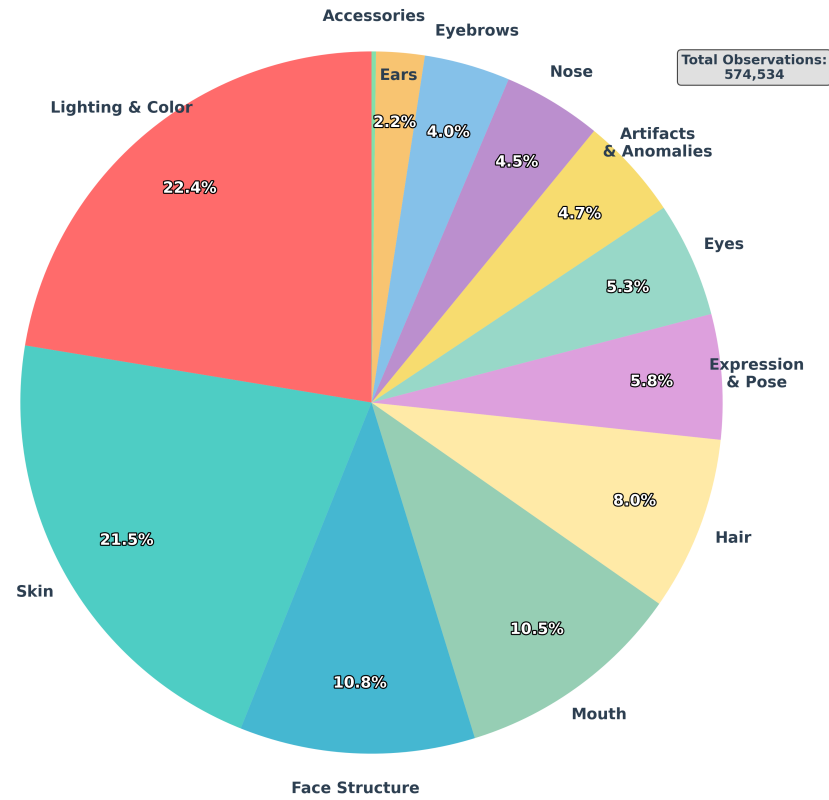


Figure 4: Distribution of deepfake detection features by category in the DF-R5 dataset (total of 574,534 feature observations), distilled from Gemini.

A.2 ANALYSES ON DEEPFAKE FEATURE COLLECTION

Figure 4 presents the distribution of deepfake-related features in our DF-R5 dataset, as distilled from Gemini’s annotations. The dataset contains a total of 574,534 feature observations spanning diverse facial and contextual attributes. The most frequently mentioned categories are **Lighting & Color** (22.4%) and **Skin** (21.5%), which together account for nearly half of all annotations. This indicates that color tone mismatches, unnatural lighting, and irregular skin textures remain the most salient artifacts identified by Gemini. Other prominent categories include **Face Structure** (10.8%), **Mouth** (10.5%), and **Hair** (8.0%), which correspond to fine-grained facial details that are particularly sensitive to generative inconsistencies. Smaller proportions are attributed to features such as **Eyes** (5.3%), **Nose** (4.5%), **Eyebrows** (4.0%), and **Ears** (2.2%), as well as higher-level attributes like **Expression & Pose** (5.8%), **Artifacts & Anomalies** (4.7%), and **Accessories** (0.2%). These occur less frequently either due to their relatively small size in the image or the semantic complexity required to identify them. Overall, the distribution indicates that MLLMs capture a diverse range of deepfake characteristics, with **Lighting & Color** and **Skin** being the most prominent and error-prone regions in deepfake generation.

Table 9: List of 74 forensic-relevant features for deepfake detection.

Index	Feature Name
1	Inconsistent pupil shape, size, or symmetry.
2	Unnatural or missing eye specular highlights (catchlights).
3	Irregular or unnatural iris detail, pattern, or color.
4	Sclera (whites of eyes) with unnatural color, brightness, or texture.
5	Asymmetric or unnatural eyelid shape or creases.
6	Misaligned eye gaze direction.

Continued on next page

Table 9 – continued from previous page

Index	Feature Name
7	Unnatural or blocky eyelashes.
8	Anomalies in eye structure (e.g., double irises/pupils, artificial tear ducts).
9	Unnatural skin texture (e.g., overly smooth, plastic-like, rough, lack of detail).
10	Inconsistent skin texture or detail across different facial regions.
11	Lack of realistic skin pores or inconsistent pore distribution.
12	Repetitive patterns in skin texture.
13	Unnatural or inconsistent skin tone or color patches.
14	Skin color mismatch between the face and neck, ears, or surrounding body.
15	Unnatural shininess, glossiness, or lack of expected specular highlights on skin surface.
16	Missing, unnatural, or misplaced blemishes, moles, scars, or freckles.
17	Unnatural or inconsistent wrinkles, folds, or creases.
18	Overexposed or underexposed skin patches.
19	Color banding or pixel noise in skin areas.
20	Lack of natural micro-variations in skin appearance.
21	Teeth with unnatural uniformity (shape, size, color, alignment, brightness).
22	Incorrect number or shape of visible teeth.
23	Teeth blending unnaturally into lips or gums, or unnatural gum line/spacing.
24	Pixelated, stretched, smudged, or artifact-laden teeth.
25	Unnatural lip contour, shape, or symmetry.
26	Unnatural lip color, texture, or color bleeding.
27	Sharp or unnatural corners of the mouth.
28	Unnatural transition between lips and teeth or inner mouth.
29	Unrealistic or missing tongue (if visible).
30	Missed philtrum (groove above upper lip).
31	Unnatural nose shape, proportions, or structural detail.
32	Asymmetric, smudged, or poorly defined nostrils.
33	Incorrect or missing shadows cast by the nose.
34	Overly smoothed nasal bridge.
35	Unnatural or asymmetric ear shapes or structures.
36	Ears inconsistent in size or position relative to the face.
37	Unnatural ear lobe attachment or blending.
38	Misaligned, asymmetric, or incomplete eyebrows.
39	Eyebrows blending unnaturally with skin or hair.
40	Unusual eyebrow thickness variation or shape.
41	Artificial, unnatural, sharp, or irregular hairline.
42	Unrealistic hair strand flow, shape, texture, or detail.
43	Hair blending unnaturally with the background or skin.
44	Artifacts, smudging, or unnatural uniformity in facial hair (beard/mustache/stubble).
45	Artificial blending or artifacts at hair roots.
46	Excessive or unnatural facial symmetry or asymmetry beyond natural variation.
47	Disproportionate facial features or overall distortion of facial structure/proportions.
48	Misaligned facial landmarks or features shifted off anatomical norms.
49	Lack of realistic depth or 3D appearance in facial structure.
50	Unnatural or overly defined cheekbone highlights or shadows.
51	Blurry, jagged, or wavy jawline edges or unnatural curvature.
52	Lack of definition in underlying bone or muscle structure relative to apparent age/body type.
53	Flat or unrealistic dimples.
54	Artificially thickened neck structure.
55	Inconsistent lighting direction or quality on different parts of the face or relative to the environment.
56	Shadows that contradict scene lighting, are missing, or unnaturally placed on the face.
57	Facial highlights (not specular) in incorrect positions or unnaturally placed.
58	Blurry, poorly defined, or overly sharp facial boundaries (face/neck, face/hair, face/background).

Continued on next page

Table 9 – continued from previous page

Index	Feature Name
59	Visible blending artifacts, seams, ghosting, or glitch-like artifacts near facial edges or transitions.
60	Incorrect or missing reflections, warping, or distortion in glasses or other transparent objects near the face.
61	Missing, distorted, or misaligned jewelry, earrings, or other accessories.
62	Clothing textures blending unnaturally into facial skin or boundaries.
63	Background distortion, anomalies, or inconsistencies near the face or head.
64	Inconsistent image resolution, pixelation, or sharpness between the face and surroundings.
65	Inconsistent noise pattern or grain level between the face and rest of the image.
66	Overall color palette, white balance, or color fringing/halos inconsistent with the environment or rest of the image.
67	Repeating elements within features (not limited to skin texture).
68	Lack of realistic depth of field effects on facial elements.
69	General artifacts or visual noise not specific to a feature.
70	Unrealistic, frozen, rigid, or unnatural facial expressions.
71	Facial expression inconsistent with other features, context, or situation.
72	Unnatural stretching or distortion of features during apparent expression.
73	Facial pose or orientation inconsistencies.
74	Unnatural makeup patterns that appear digitally applied or inconsistent.

A.3 PROMPTS FOR DATASET GENERATION

In this section, we provide the full prompts used in our feature discovery (step 1), feature scoring (step 2), and reasoning generation processes (step 3). In step 1, we use the prompt in Figure 5 to generate $K = 50$ distinct visual characteristics from each of the four MLLMs (Gemini 2.5, GPT-4o, Qwen 2.5-Max, and LLaMA 4 Maverick). We then consolidate the $4 \times K = 200$ features into a unified list using the prompt in Figure 6. The final set of 74 consolidated features is reported in Table 9. In step 2, we use the prompt in Figure 7 to systematically score each of the $k = 74$ consolidated features for every image. Finally, in step 3, we use the prompt in Figure 8 to group the real-indicative features into logical categories and provide reasoning for each group.

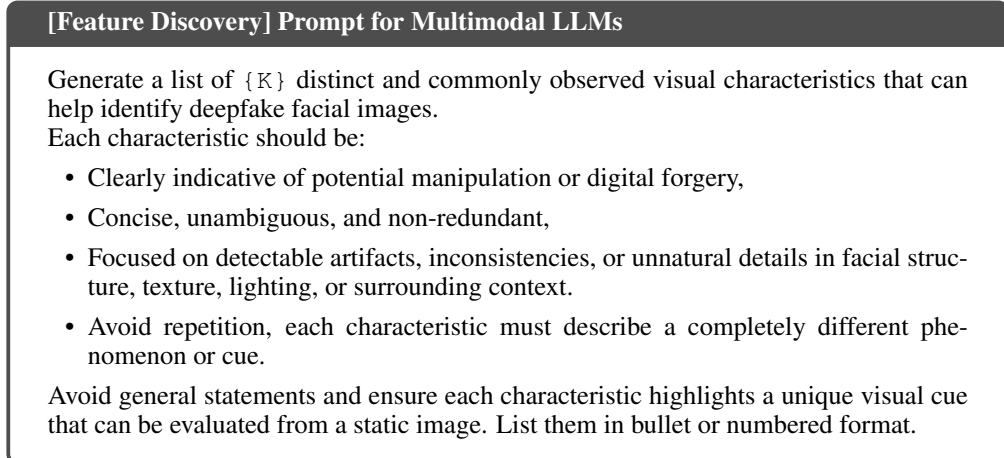


Figure 5: Prompt for generating a comprehensive set of visual cues to identify deepfake facial images, used across Gemini, GPT, LLaMA, and Qwen.

[Feature Discovery] Feature Consolidation Prompt for Multimodal LLMs

You are provided with a list of the top $\{K\} \times 4 = \{4 \times K\}$ common forensic-relevant features used to detect forgery in facial images, as analyzed by state-of-the-art large language models, including GPT-4o, Gemini 2.5 Flash, Qwen 2.5-Max, and LLaMA 4 Maverick.

Your task is to:

1. Combine all $\{K\} \times 4 = \{4 \times K\}$ features across these models into a single unified list.
2. Eliminate duplicate or overlapping features to ensure clarity and uniqueness.
3. Ensure each feature:
 - Is clearly defined and focused on detecting forgery in visual facial content.
 - Reflects diversity across models but avoids any redundancy.
 - Maintains precise and non-ambiguous language.

Output format:

A final list of unique and consolidated features, each on a separate line, numbered from 1 to N.

The provided features are:

GPT-4o: {features_gpt}

Gemini 2.5: {features_gemini}

Qwen 2.5: {features_qwen}

LLaMA 4: {features_llama}

Figure 6: Prompt for consolidating $4 \times K$ (e.g., 4×50) forensic-relevant features into a unified and non-redundant list, used across GPT-4o, Gemini 2.5, Qwen 2.5, and LLaMA 4.

A.4 PROMPT FOR QUALITATIVE EVALUATION

We provide the full prompt used to evaluate the quality of reasoning responses from different models in Figure 9.

Table 10: Comprehensive detection performance (%) of our method compared with deepfake detection baselines across five domains.

Method	→ DDIM				→ PixArt				→ SD2.1			
	Acc	Prec	Rec	F1	Acc	Prec	Rec	F1	Acc	Prec	Rec	F1
LLaVA	63.30	88.78	34.67	49.86	70.90	91.86	50.84	65.46	53.30	80.00	15.91	26.54
DE-FAKE	46.30	40.63	4.95	8.83	86.30	91.42	81.99	86.45	95.40	92.43	99.43	95.80
FakeShield	44.51	35.66	44.51	31.84	88.70	89.59	88.70	88.57	92.30	92.48	92.30	92.28
UnivCLIP	77.61	86.88	80.63	74.85	82.20	93.31	74.09	89.31	76.70	88.39	78.81	74.81
SIDA	71.46	79.34	72.66	70.07	68.00	65.41	84.80	73.86	92.41	92.42	92.33	92.37
DX-LLaVA (ours)	92.60	99.11	86.43	92.34	84.60	100.00	71.11	83.11	89.70	99.53	81.06	89.35
DPRPO (ours)	95.80	98.79	93.14	95.88	88.60	99.29	79.17	88.10	94.80	96.67	93.37	94.99
Method	→ SiT				→ StyleGAN3				Average			
	Acc	Prec	Rec	F1	Acc	Prec	Rec	F1	Acc	Prec	Rec	F1
LLaVA	50.90	64.71	8.71	15.36	67.10	88.93	41.97	57.03	61.10	82.86	30.42	42.85
DE-FAKE	49.70	54.55	2.38	4.55	79.60	94.58	64.22	76.50	71.46	74.72	50.59	54.43
FakeShield	49.70	75.05	49.70	33.22	98.70	98.72	98.70	98.70	74.78	78.30	74.78	68.92
UnivCLIP	61.31	71.53	83.03	40.01	81.61	92.45	76.39	86.46	75.89	86.51	78.59	73.09
SIDA	56.29	76.55	56.72	46.53	95.01	95.19	94.91	94.98	76.63	81.78	80.28	75.56
DX-LLaVA (ours)	57.20	100.0	15.25	26.46	99.10	99.22	99.03	99.13	84.64	99.57	70.58	78.08
DPRPO (ours)	66.60	63.01	81.98	71.26	99.30	99.23	99.42	99.32	89.02	91.40	89.42	89.91

[Feature Scoring] Feature Scoring Prompt for Gemini

Given the attached image, evaluate each of the $\{k\}$ listed deepfake characteristics. For each characteristic, respond with:

- Real (-1) if the characteristic appears natural,
- Fake (+1) if the characteristic clearly indicates digital forgery or manipulation,
- Uncertain (0) if the characteristic cannot be clearly evaluated from the provided image.

Provide your answers in the following format:

```
{feature 1: <score>},
{feature 2: <score>},
...
{feature k: <score>}.
```

Finally, based on your evaluation, provide your overall judgment clearly as:

Final Answer: <real/fake>

Note that your score of each feature should be fair, independent marking without bias.

Figure 7: Prompt for systematic scoring of $k = 74$ forensic-relevant characteristics in deepfake images, requiring per-feature evaluation and a final overall decision.

A.5 DETAILED COMPUTATION OF PREDICTION CONSISTENCY REWARD (PCR)

The Prediction Consistency Reward is computed through paragraph-level evidence scoring. Each paragraph is analyzed using dictionaries of real terms \mathcal{R} , fake terms \mathcal{F} , and negation terms \mathcal{N} to determine whether it supports a “real” or “fake” label. Scores are accumulated based on the frequency of matched terms, and a label is assigned accordingly. All paragraphs contribute to a majority vote, producing the majority label a_{maj} . The reward is set high when the majority label matches the final answer a_{final} , and reduced when inconsistencies are detected. The detailed procedures are presented in Algorithms 1, 2, and 3. This reward design enforces consistency between the final answer and the majority of paragraph-level predictions, thereby improving the reliability of the model’s outputs.

Algorithm 1 Prediction Consistency Reward Computation

```

1: Input: paragraph index  $i$ , paragraph  $p_i$ , all paragraphs  $\mathcal{P}$  in  $L$  samples, final answer  $a_{\text{final}}$ , number of
   paragraphs  $V$ , majority answer  $a_{\text{maj}}$ , prediction consistency reward  $r_i$ 
2: Compute paragraph scores:  $u_i \leftarrow \text{score\_paragraph}(p_i)$ 
3: Predict label:  $\hat{y}_i \leftarrow \text{predict\_label}(u_i)$ 
4: if  $p_i$  is the final answer paragraph then
5:   Initialize:  $V_{\text{real}} \leftarrow 0$ ,  $V_{\text{fake}} \leftarrow 0$ 
6:   for  $j = 1$  to  $i - 1$  do
7:      $u_j \leftarrow \text{score\_paragraph}(p_j)$ 
8:      $\hat{y}_j \leftarrow \text{predict\_label}(u_j)$ 
9:     if  $\hat{y}_j = \text{"real"}$  then
10:       $V_{\text{real}} \leftarrow V_{\text{real}} + 1$ 
11:    else if  $\hat{y}_j = \text{"fake"}$  then
12:       $V_{\text{fake}} \leftarrow V_{\text{fake}} + 1$ 
13:    end if
14:   end for
15:   if  $V_{\text{real}} > V_{\text{fake}}$  then
16:      $a_{\text{maj}} \leftarrow \text{"real"}$ 
17:   else if  $V_{\text{fake}} > V_{\text{real}}$  then
18:      $a_{\text{maj}} \leftarrow \text{"fake"}$ 
19:   else
20:      $a_{\text{maj}} \leftarrow a_{\text{final}}$ 
21:   end if
22:   if  $a_{\text{maj}} = a_{\text{final}}$  then
23:      $r_i \leftarrow 1.0$ 
24:   else
25:      $r_i \leftarrow 0.0$ 
26:   end if
27: else
28:    $r_i \leftarrow 1.0$ 
29: end if
30: Return:  $r_i$ 

```

Algorithm 2 Paragraph Scoring Function (score_paragraph)

```

1: Input: Paragraph text  $p$ 
2: Initialize:  $s_{\text{real}} \leftarrow 0.0$ ,  $s_{\text{fake}} \leftarrow 0.0$ 
3: Declare real patterns  $\mathcal{R}$ , fake patterns  $\mathcal{F}$ , negation patterns  $\mathcal{N}$ 
4: for each real term match in  $p$  do
5:   if a negated term exists then
6:      $s_{\text{fake}} \leftarrow s_{\text{fake}} + 1$ 
7:   else
8:      $s_{\text{real}} \leftarrow s_{\text{real}} + 1$ 
9:   end if
10: end for
11: for each fake term match in  $p$  do
12:   if a negated term exists then
13:      $s_{\text{real}} \leftarrow s_{\text{real}} + 1$ 
14:   else
15:      $s_{\text{fake}} \leftarrow s_{\text{fake}} + 1$ 
16:   end if
17: end for
18: Return:  $\{s_{\text{real}}, s_{\text{fake}}\}$ 

```

Algorithm 3 Predict Label from Paragraph Scoring (predict_label)

Require: Paragraph text p
Ensure: Predicted label $\ell \in \{\text{"real"}, \text{"fake"}\}$

```

1: if  $s_{\text{real}} \geq s_{\text{fake}}$  then
2:    $\ell \leftarrow \text{"real"}$ 
3: else
4:    $\ell \leftarrow \text{"fake"}$ 
5: end if
6: return  $\ell$ 

```

[Reasoning Generation] Grouping and Reasoning Prompt for Deepfake Features

Analyze the provided image, which has `{n_features}` features which indicate that the image is `{label}`.

Your task is to first group these features into a maximum of `{M}` logical groups based on their conceptual similarity. Then, for each group, provide a concise reasoning that explains what the features within that group collectively suggest about the authenticity of this specific image. Instead of defining the features in general, describe what is notable or unusual (if the image is “fake”) or typical (if the image is “real”) about these features in the context of the image.

The features indicating the image is `{label}` are:

- `{feature 1}`
- `{feature 2}`
- ...
- `{feature n_features}`

The ground truth label for this image is: `{label}`

Please provide your analysis in JSON format following this exact structure:

```
{
  "groups": {
    "group_name_1": ["feature_name_a", "feature_name_b", ...],
    "group_name_2": ["feature_name_c", "feature_name_d", ...],
    ...
  },
  "group_name_1": "reasoning for group 1",
  "group_name_2": "reasoning for group 2",
  ...
  "answer": "ground truth label"
}
```

Figure 8: Prompt for grouping real-indicative features into logical categories with reasoning. Each image has different variables (e.g., `n_features`, `M`, `label`, and the list of features).

Evaluation Prompt

You are an expert evaluator for deepfake detection responses. Your task is to evaluate a given response to an image across five critical dimensions for deepfake detection accuracy and reliability.

Scoring Scale: For each dimension, assign an integer score from **0 to 5**:

- 0 = Very poor / completely incorrect
- 1 = Poor
- 2 = Fair
- 3 = Good
- 4 = Very good
- 5 = Excellent

Evaluation Dimensions

1. **Classification Accuracy & Consistency:**

Does the response correctly classify the image as real or fake?

Is the classification consistent with both the ground truth and the reasoning provided?

2. **Reasoning Quality:**

Does the response provide a logical, step-by-step explanation of its decision?

Is the reasoning free from contradictions or irrelevant details?

3. **Evidence Grounding & Image Alignment:**

Does the response cite specific visual artifacts that are actually present in the image?

Does it avoid hallucinations (mentioning features not visible)?

4. **Confidence Calibration:**

Is the expressed confidence level appropriate given the clarity of evidence in the image?

Does the response avoid overstating or understating certainty?

5. **Clarity & Usefulness:**

Is the response clear, well-structured, and easy to understand?

Would it be useful for a human investigator verifying deepfake authenticity?

Output Format

Respond strictly in JSON with this structure:

```
{
  "classification_accuracy": <0-5>,
  "evidence_grounding": <0-5>,
  "reasoning_quality": <0-5>,
  "confidence_calibration": <0-5>,
  "clarity_usefulness": <0-5>,
  "justification": "<concise explanation of the scoring rationale>"
}
```

Evaluation Task

Now evaluate the given image with the following details:

Response: {response}

Prediction: {prediction}

Ground Truth: {ground_truth}

Figure 9: Prompt provided to evaluators for scoring deepfake detection responses on a 0-5 scale across five criteria.